ChemCommun

FEATURE ARTICLE

Synthetic Approaches to Construct Viral capsid-like Spherical Nanomaterials

Kazunori Matsuura*[a,b]

Received 00th January 20xx,
Accepted 00th January 20xx

DOI: 10.1039/x0xx00000x

www.rsc.org/

This feature article describes recent progress in synthetic strategies to construct viral capsid-like spherical nanomaterials using the self-assembly of peptides and/or proteins. By mimicking the self-assembly of spherical viral capsids and clathrin, trigonal peptide conjugates bearing β-sheet-forming peptides, glutathiones, or coiled-coil-forming peptides were developed to construct viral capsid-like particles. β-Annulus peptides from tomato bushy stunt virus self-assembled into viral capsid-like nanocapsules with a size of 30–50 nm, which could encapsulate various guest molecules and be decorated with different molecules on their surface. Rationally designed fusion proteins bearing symmetric assembling units afforded precise viral capsid-like polyhedral assemblies. These synthetic approaches to construct artificial viruses could become useful guidelines to develop novel drug carriers, vaccine platforms, nanotemplates and nanoreactors.

1. Introduction

A virus is an infective molecular assembly with a diameter of 20–250 nm, which can reproduce itself in living host cells. Natural viruses can be classified by their morphologies in spherical (e.g. human papillomavirus), rod-like (tobacco mosaic virus), envelope-type (influenza virus, HIV) and complex-type viruses (bacteriophage T4).[1] Simple viruses, such as spherical and rod-like viruses, possess supramolecular structures consisting of genome nucleic acids encapsulated in self-assembled coat proteins called 'capsids'. Capsid proteins of rod-like viruses form helical assemblies along the nucleic acid, while capsid proteins of spherical viruses form capsule structures with icosahedral symmetry.[1-5] The number and arrangement of capsid proteins of spherical viruses are related to the triangulation number (*T* number), which is derived from quasi-equivalence theory (Figure 1A). The different letters (A–D) in Figure 1A denote different conformations of the same capsid protein. The *T* number usually refers to the number of unique/distinct structural environments or simply to the number of coat protein subunits present in an icosahedral asymmetric unit. Thus, most spherical viruses are formed by the self-assembly of multiples of 60 proteins ($T \times 60$), which have an icosahedral symmetry including quasi-six-fold (threefold), fivefold and twofold symmetric axes. For example, the minute virus of mice (MVM, $T = 1$) capsid consists of 60 equivalent protein subunits,[6] The tomato bushy stunt virus (TBSV, $T = 3$) capsid consists of 180 quasi-equivalent protein subunits[7, 8] and the *Nudaurelia capensis* ω virus (NωV, $T = 4$) capsid consists of 240 quasi-equivalent protein subunits (Figure 1B).[9] There are also nonviral capsids formed by protein self-assembly in nature. *Aquifex aeolicus* lumazine synthase (AaLS) is an example of a nonviral, naturally empty dodecahedral capsid with a size of 16 nm (Figure 1B).[10] The clathrin lattice is a polyhedral structure with a size of about 100 nm, self-assembled from clathrin triskelion in the presence of Mg^{2+} ions.[11, 12] Recently, the self-assembly pathways of several viral capsids were revealed by mass spectroscopy, atomic force microscopy and electron microscopy.[13-16] It was found that trimeric and/or pentameric

[a] *Department of Chemistry and Biotechnology, Graduate School of Engineering, Tottori University, Tottori 680-8552, Japan. E-mail: ma2ra-k@tottori-u.ac.jp.*
[b] *Centre for Research on Green Sustainable Chemistry, Tottori University*

K. Matsuura

Kazunori Matsuura obtained his Ph.D. from Tokyo Institute of Technology in 1996 and then joined the Department of Molecular Design and Engineering at Nagoya University as an Assistant Professor. In 2001, he moved to the Department of Chemistry and Biochemistry at Kyushu University, where he served as an Associate Professor. In 2006, he was selected as a researcher for the JST PRESTO project "Structure Control and Function." Since 2012, he has been working as a Full Professor at the Department of Chemistry and Biotechnology at Tottori University. Prof. Matsuura received The Young Scientists' Prize from the Minister of Education, Culture, Sports, Science and Technology in 2008, the JSPS Prize from the Japan Society of the Promotion of Science in 2012, and The Chemical Society of Japan Award for Creative Work in 2016.

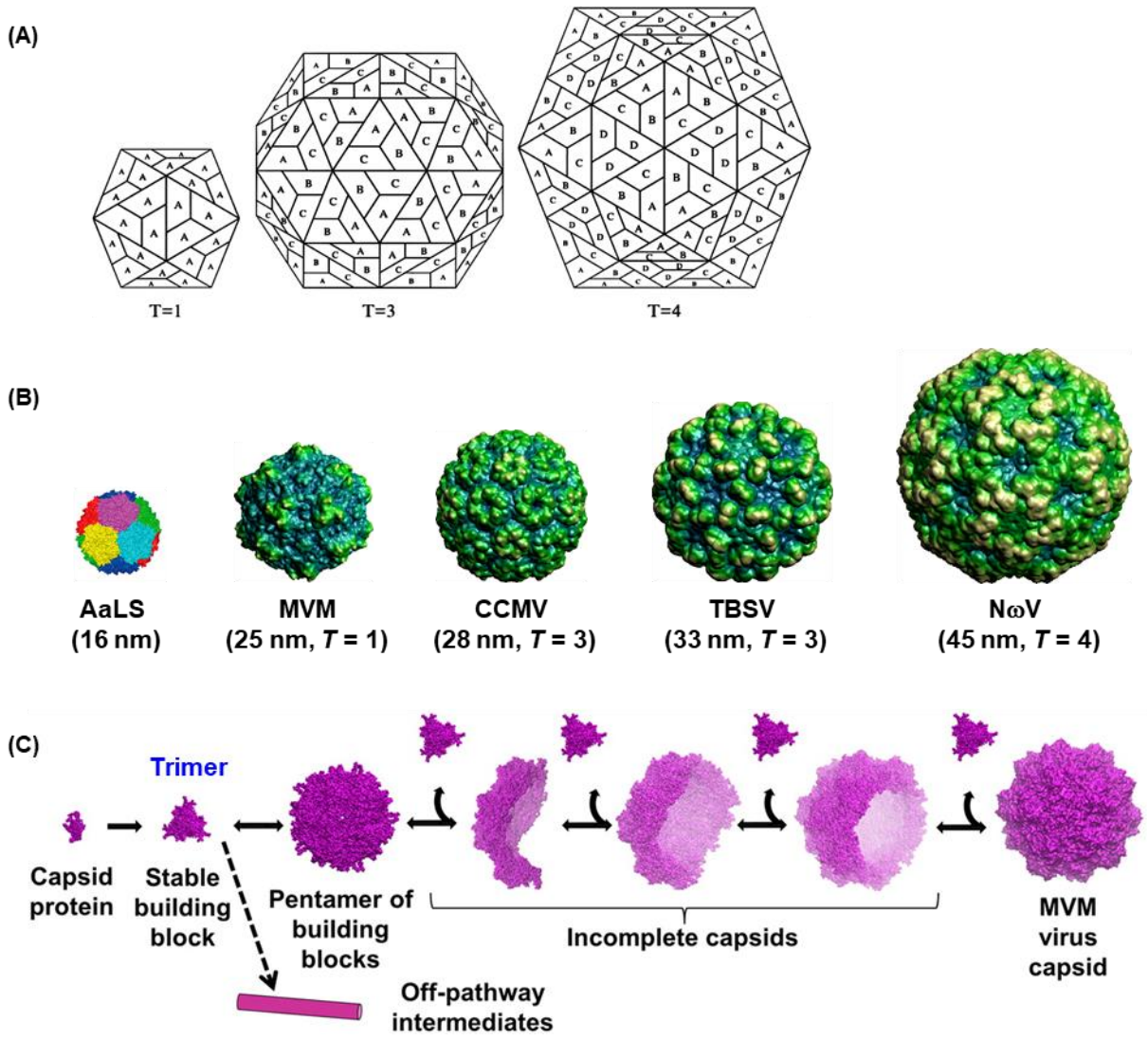

Fig. 1 Structures and self-assembly of spherical viral capsids. (A) Illustration of icosahedral assemblies of capsid proteins with different triangulation numbers, where different letters denote different conformations of the same capsid protein (Reproduced with permission from ref. 5. Copyright 2008, Elsevior). (B) Comparison of the sizes of several spherical viruses (PDB entry: 1MVM, 1CWP, 2TBV, and 1OHF) and *Aquifex aeolicus* lumazine synthase (AaLS, PDB entry: 1HQK). (C) Schematic model of the self-assembly of MVM capsid (Reproduced with permission from ref. 15. Copyright 2016, American Chemical Society).

intermediates consisting of capsid proteins existed in these pathways.

Over the past three decades, viral capsids have been recognised as attractive organic materials possessing discrete size, unique morphology, constant aggregation number and good cell-transfection ability. Thus, these materials have been utilised as carriers for drug delivery and as platforms for vaccine materials.[17-21] In 1998, Douglas and co-workers demonstrated the mineralisation of polyoxometalates and the encapsulation of an anionic polymer in a cowpea chlorotic mottle virus (CCMV) capsid. At that time, the researchers suggested a new perspective on how to apply spherical viral capsids as nanocarriers and nanoreactors (Figure 2A),[22] and since then , bio-nanotechnology utilising viral capsids has evolved considerably.[23-28] For example, the encapsulation of inorganic nanoparticles (Figure 2B),[29-31] enzymes (Figure 2C),[32-36] fluorescence proteins (Figure 2D)[37-41] and synthetic polymers[42] into spherical viral capsids and viral capsid-like lumazine synthase (AaLS) has been reported in several studies. Surface decoration of spherical viral capsids with functional materials such as conductive nanoparticles (Figure 2E),[43] DNA aptamers (Figure 2F)[44, 45] and oligosaccharides[46, 47] has also been reported. The natural and mutated viral capsids applied to bio-nanotechnology can be produced by overexpression of the viral genome in the host. The construction of 'tailor-made' viral capsid-like nanocapsules from rationally designed synthetic molecules would notably contribute to advances in the bio-nanotechnology field. The viral capsid-like nanocapsules are defined as spherical materials self-assembled from rationally designed peptide/protein with diameters of 20-250 nm having hollow inside, relative narrow size distribution, and roughly constant aggregation number. The formation of viral capsid-like

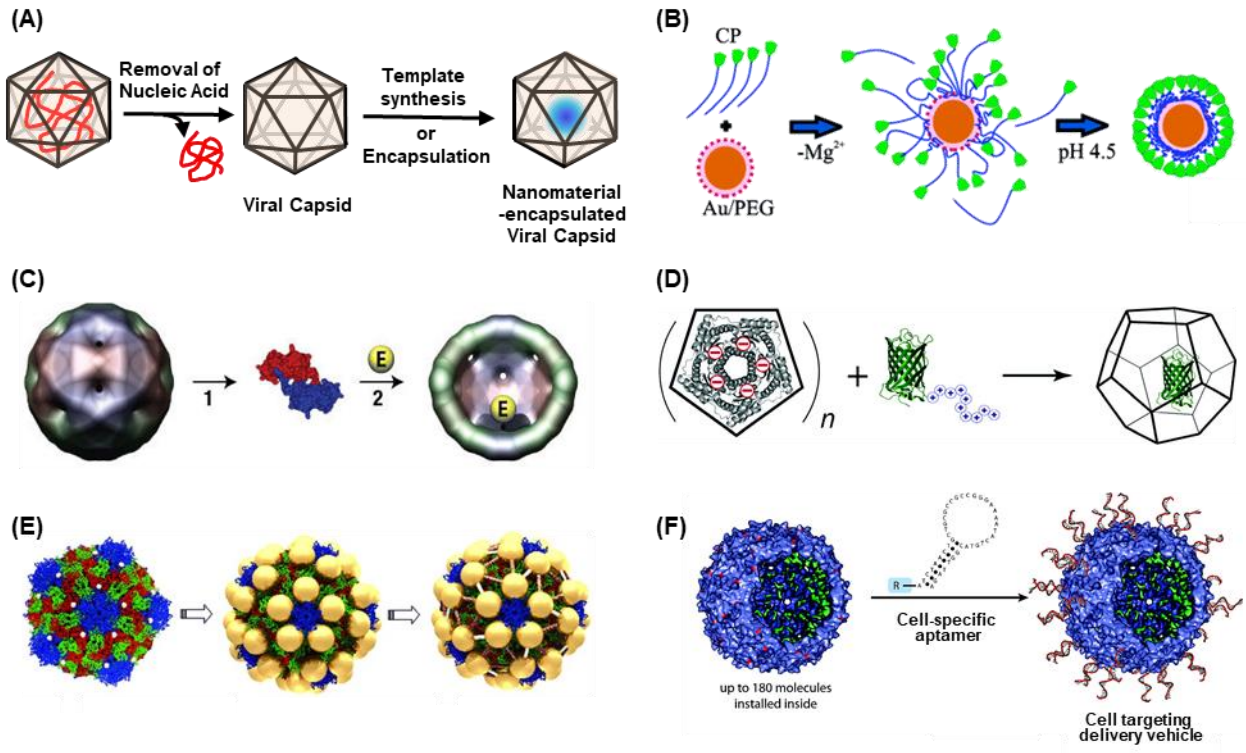

Fig. 2 Applications of spherical viral capsids in bio-nanotechnology. (A) Schematic illustration of the encapsulation of nanomaterials into viral capsids. (B) Encapsulation of an Au nanoparticle (AuNP) into a brome mosaic virus capsid (Reproduced with permission from ref. 30. Copyright 2006, American Chemical Society). (C) Encapsulation of horse radish peroxidase into a CCMV capsid (Reproduced with permission from ref. 32. Copyright 2007, Springer Nature). (D) Encapsulation of green fluorescence protein (GFP) into an AaLS capsid (Reproduced with permission from ref. 37. Copyright 2006, American Chemical Society). (E) Decoration of AuNPs onto a cowpea mosaic virus (CPMV) capsid (Reproduced with permission from ref. 43. Copyright 2005, John Wiley and Sons). (F) Decoration of DNA aptamers on a CPMV capsid (Reproduced with permission from ref. 44. Copyright 2009, American Chemical Society).

nanocapsules is based on interactions among polypeptides, such as hydrogen bonds, electrostatic, π–π stacking and hydrophobic interactions, which is different from assembling mechanism of micelles and vesicles from amphiphilic molecules. However, the chemical strategies to create viral capsid-like assemblies from synthetic molecules are still at an early stage.[48]

Fujita and co-workers developed many coordination cages with sizes of 3–8 nm, which were self-assembled from rationally designed organic ligands and palladium ions in water.[49] However, the size of these coordination cages was evidently smaller than that of natural spherical viruses. For example, $M_{12}L_{24}$ coordination cages were constructed by the self-assembly of 12 Pd^{2+} ions and 24 bidentate ligands, and these structures were able to encapsulate ubiquitin, a small protein.[50] Recently, the researchers succeeded in constructing $M_{30}L_{60}$ icosadodecahedron cages with a diameter of 8.2 nm, which consisted of 30 Pd^{2+} ions and 60 bidentate ligands.[51]

DNA is promising as a scaffold for constructing virus-sized nanoarchitectures.[52, 53] We previously demonstrated that a DNA three-way junction bearing self-complementary sticky ends can be self-assembled into spherical DNA assemblies (nucleo-spheres) with sizes depending on the DNA concentration.[54-58] Joyce and co-workers demonstrated that a designed long single-stranded DNA spontaneously folded to form octahedral structures with a size of 22 nm.[59] Mao and co-workers reported that three-point-star DNA motifs could be self-assembled into tetrahedral (10 nm), dodecahedral (24 nm) or buckyball (42 nm) structures by controlling the flexibility and concentration of the material.[60] Although these discrete, virus-sized DNA nanostructures are interesting, applying diverse functions to their surface might be restricted by a polyanionic charge.

In contrast, diverse surface functions can be designed on peptide/protein assemblies, and to date, various artificial peptide/protein assemblies have been developed by the rational design of ligand–receptor interactions and domain swapping between two proteins, and secondary structure such as β-sheet and α-helix coiled-coil.[61-68] The advantage of construction of nanostructures using peptide/protein is that they have a relatively rigid conformation and diverse surface properties such as cation, anion, hydrophilic and hydrophobic properties. The secondary structure formation of designed peptide/protein assemblies can be predicted from the primary sequence, so that the self-assembly process can be programmed. This feature article outlines recent progress in synthetic approaches to construct viral capsid-like spherical nanomaterials, especially using peptide/protein self-assembly.

2. Viral capsid-like particles self-assembled from amphiphilic macrocycles

Calix[n]arenes and calix[n]resorcarenes are known as cone-shaped macrocyclic host molecules having a relatively small cavity.[69] These cone-shaped macrocycles function not only as selective receptors for various small guest molecules, but also as components of molecular assemblies.[70] For example, Sakurai and co-workers demonstrated that calix[4]arene amphiphiles self-assembled into monodisperse micelles with discrete aggregation numbers whose values could be chosen between 6, 8, 12, 20 and 32 (Figure 3A).[71] Since some of these numbers coincide with the face numbers of Platonic solids, they were named 'Platonic micelles'. Mendoza and co-workers reported the self-assembly of conically shaped carboxylic acid derivatives of calix[4]arene and calix[5]arene with uranyl cations UO_2^{2+} to afford octahedral and icosahedral metallocages.[72]

Aoyama and co-workers developed calix[4]resorcarene-based macrocyclic amphiphiles bearing eight disaccharide moieties (maltose, cellobiose or lactose) and four long-alkyl chains (Figure 3B).[73-77] The glycocluster amphiphiles formed stable 5-nm micellar nanoparticles (glyco-nanoparticles) having an aggregation number of about 6. The glyco-nanoparticles agglutinated with Na_2HPO_4 via sugar-to-phosphate hydrogen bonding.[75] The facile phosphate complexation of glyco-nanoparticles suggests their potential application as a new type of DNA binder, especially as gene carriers.[76] Indeed, glyco-nanoparticles bearing cellobioses can be co-assembled with plasmid DNA pCMVluc (7040 bp) in a number-, size- and shape-controlled manner to give artificial 'glycoviruses' of about 50 nm in diameter (Figure 2B). The surface ζ-potential of glyco-nanoparticles bearing cellobioses complexed with plasmid DNA was about 0 mV, indicating a dense glyco-nanoparticles coating on the surface. Cellobiose-containing glycoviruses with a viral size of about 50 nm functioned as effective gene carriers for HeLa cells based on size-dependent endocytosis, whereas the transfection ability of maltose- and lactose-bearing glycoviruses with a size of 200–300 nm was low.[77] In contrast, lactose-bearing glycoviruses were well transfected into HepG2 cells, which possess galactose-receptors, by receptor-mediated endocytosis. This pioneering work by Aoyama and co-workers opened the door to a new research field on 'artificial viruses'.

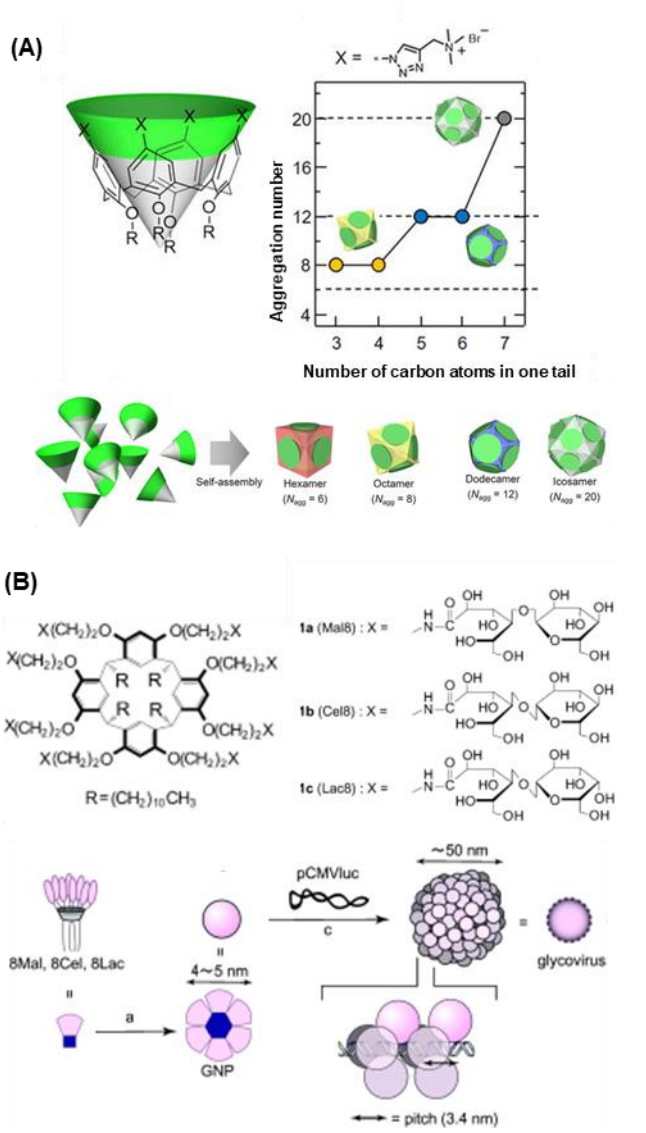

Fig. 3 (A) Platonic micelles self-assembled from calix[4]arene amphiphiles (Reproduced with permission from ref. 71). (B) Hierarchical growth of a calix[4]resorcarene amphiphile bearing disaccharides through nanoparticle (GNP) to glycovirus (Reproduced with permission from ref. 73. Copyright 2004, John Wiley and Sons).

3. Viral capsid-like particles self-assembled from trigonal peptide conjugates

3-1. Trigonal β-structure-forming peptide assemblies

As mentioned above, natural spherical viral capsids with icosahedral symmetry can be spontaneously formed by self-assembly of proteins via threefold and fivefold symmetric protein oligomer intermediates.[2-5] The clathrin lattice also self-assembles from a threefold symmetric clathrin triskelion consisting of three proteins in the presence of Mg^{2+} ions, which participate in receptor-mediated endocytosis.[11, 12] Viral and clathrin self-assembly is based on threefold symmetric structures with directed intermolecular interactions, which serve as a model for the design of artificial viral capsid-like nanoparticles. The threefold symmetric pre-organisation of peptide chains allows one to reduce the entropy loss during the self-assembling process and enables the formation of unique assemblies in water.

In 2005, we first demonstrated the self-assembly of an artificial trigonal peptide conjugate containing three β-sheet-forming peptides [Trigonal$(FKFE)_2$] into viral capsid-like nanoparticles (Figure 4A).[78] Trigonal$(FKFE)_2$ was synthesised by coupling the thiol groups of anti-parallel β-sheet-forming peptides (CFKFEFKFE) with threefold symmetric iodoacetamide-treated core molecules. Circular dichroism (CD) and Fourier-transform infrared (FTIR) spectroscopy studies of an acidic aqueous solution of Trigonal$(FKFE)_2$ showed the formation of an

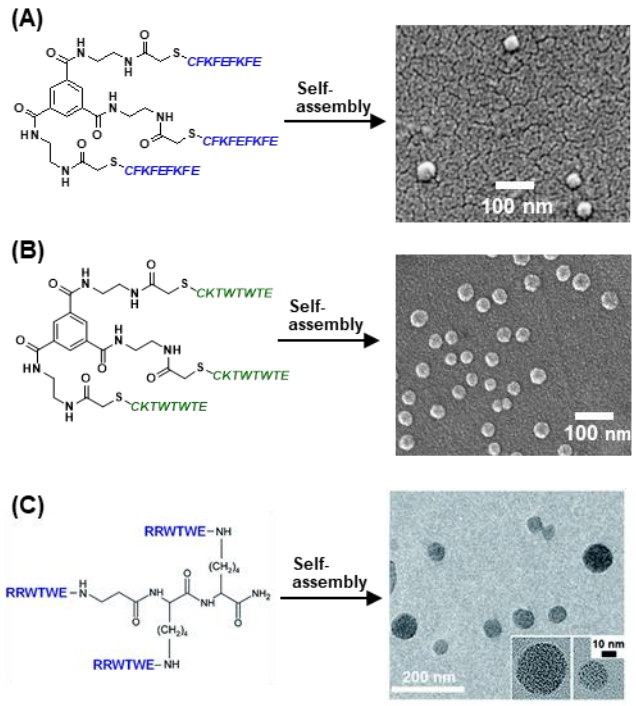

Fig. 4. Peptide nanospheres self-assembled from trigonal conjugates of β-structure-forming peptides. (A) Trigonal(FKFE)$_2$ (Reproduced with permission from ref. 78. Copyright 2005, American Chemical Society). (B) Trigonal-WTW (Reproduced with permission from ref. 83. Copyright 2011, Royal Society of Chemistry). (C) Trigonal conjugate bearing three tryptophan zipper-forming peptides, developed by Ryadnov et al. (Reproduced with permission from ref. 84. Copyright 2016, Royal Society of Chemistry).

anti-parallel β-sheet structure, which indicates that Trigonal(FKFE)$_2$ forms intermolecular assemblies, since it is not possible for a single Trigonal(FKFE)$_2$ molecule to form such structures. Atomic force microscopy (AFM) images of Trigonal(FKFE)$_2$ on a mica substrate showed the formation of domed structures with diameters of 35–70 nm and a z-height of (2.3 ± 0.4) nm. In contrast, the component peptide CFKFEFKFE formed nanofibers with a width of about 40 nm and a z-height of about 1.0 nm. The z-heights of the Trigonal(FKFE)$_2$ assemblies on the mica substrate are twice those of peptide CFKFEFKFE nanofibers, suggesting that Trigonal(FKFE)$_2$ might form hollow nanospheres in acidic solution. Scanning electron microscopy (SEM) images of Trigonal(FKFE)$_2$ also showed the presence of spherical assemblies with sizes of 22–34 nm and concave structures with sizes of 50–100 nm, which might have been formed by collapse of the spherical assemblies on mica. The average diameter of the nanospheres in acidic solution was determined by dynamic light scattering (DLS) and was found to be (19.1 ± 4.0) nm. When two Trigonal(FKFE)$_2$ molecules form an anti-parallel β–sheet, the distance between the two core benzene rings is estimated to be about 5.8 nm from the molecular model. Assuming that the distance is a side of a dodecahedron, the diameter of the assembly is calculated to be about 16 nm for a dodecahedron structure. This estimated diameter is comparable to the average diameter of the nanospheres observed by DLS.

On the other hand, wheel-like trigonal peptide conjugates (Wheel-FKFEs) consisting of three β-sheet-forming peptides FKFECKFE were self-assembled into nanofibers with a width of 3–4 nm.[79] Apparently, the peptide units of Wheel-FKFEs in nanofibers form anti-parallel β-sheets with attractive intermolecular ionic complementarity. Since Wheel-FKFEs have the potential to limit their conformation to planar triangular structures by the formation of intramolecular salt bridges, the planarity of Wheel-FKFEs can also promote the stacking assembly.

A tryptophan zipper is a secondary structure motif that forms a stable twisted β-hairpin structure due to the interaction between tryptophan residues.[80-82] We also synthesised a trigonal peptide conjugate bearing three tryptophan zipper-forming peptides CKTWTWTE (Trigonal-WTW).[83] CD spectra showed that Trigonal-WTW formed tryptophan zipper structures at pH 7 and 11, but not at pH 3. SEM images of the conjugate showed the formation of nanospheres with a size of about 30 nm at pH 7 (Figure 4B), which is in good agreement with the average diameter obtained by DLS (19.8 ± 1.9 nm). In contrast, only irregular aggregates were observed in the SEM images at pH 3. At pH 11, a mixture of spherical assemblies with sizes of 30–50 nm and fibrous assemblies with a width of about 5 nm (beads-on-string structure) was formed. The isoelectric point (*pI*) was estimated to be 7.1, and therefore, Trigonal-WTW possesses a zwitterionic structure at pH 7. Apparently, Trigonal-WTW arranges into nanospheres by forming intermolecular anti-parallel β-sheet-like structures (including tryptophan zippers) due to an attractive ionic complementarity. In contrast, the trigonal conjugate of CKTFTFTE, in which the W of Trigonal-WTW is replaced by F, did not give a spherical structure regardless of the pH. Therefore, the formation of pH-dependent spherical structures is characteristic for Trigonal-WTW.

By adopting a similar strategy, Ryadnov and co-workers reported that a trigonal conjugate of β-Ala-Lys-Lys hub bearing three tryptophan zipper-forming peptides (RRWTWE) self-assembled into spherical capsules with a diameter of 20–200 nm (Figure 4C).[84] The peptide nanocapsules self-assembled from the trigonal conjugates can be utilised to deliver short interfering RNAs (siRNAs) to promote gene silencing in mammalian cells. Moreover, these nanocapsules showed antimicrobial activity in bacterial cultures.

3-2. Trigonal glutathione assemblies

It has been reported that even simple dipeptide and tripeptide derivatives function as self-assembly units. Gazit and co-workers found that the aromatic dipeptide FF, which is the hydrophobic core motif of β-amyloid, formed crystalline nanotube assemblies in water.[85, 86] Atkins and co-workers reported that oxidised glutathione formed fibrous assemblies in dimethyl sulfoxide to become an organogel,[87] and that a pyrene-glutathione conjugate self-assembled into a hydrogel.[88]

We found that the trigonal conjugation of glutathione (Trigonal glutathione, TG) formed spherical assemblies with

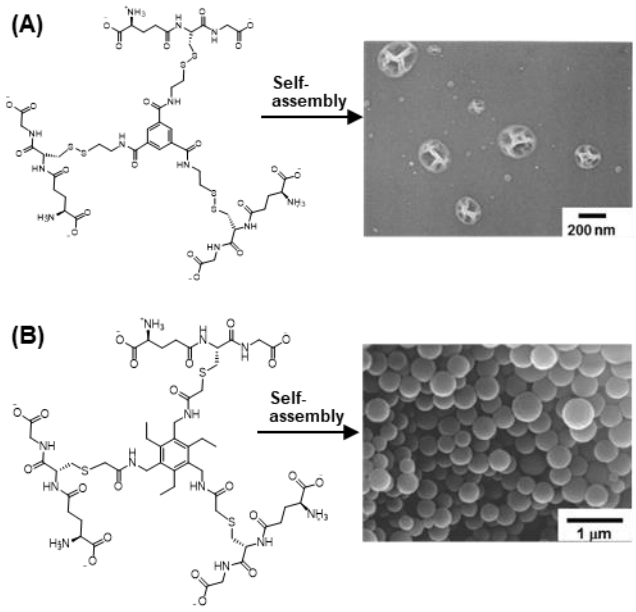

Fig. 5. Peptide nanospheres self-assembled from trigonal conjugates of glutathione. (A) Trigonal-glutathione (Reproduced with permission from ref. 89. Copyright 2009, Royal Society of Chemistry). (B) Conformation-regulated trigonal-glutathione (Reproduced with permission from ref. 91. Copyright 2010, Chemical Society of Japan).

sizes of 100–250 nm in water (Figure 5A), whereas reduced glutathione afforded only irregular aggregates in water.[89] Interestingly, the size of the assemblies was minimally affected by concentration and pH. The nanospheres underwent structural changes from hollow to filled spheres depending on the concentration. The SEM image of 1 mM TG shows the formation of wrinkly collapsed spherical assemblies (Figure 4A), suggesting the existence of a hollow interior. In contrast, hard spheres were observed in the SEM image at a higher concentration of 10 mM, suggesting the existence of filled spheres. Equilibrium dialysis experiments showed that guest molecules such as uranine were effectively encapsulated into hollow nanospheres at lower concentrations, whereas their encapsulation into filled nanospheres became more difficult at higher TG concentrations. Recombination of the disulfide bonds of the guest-encapsulated TG nanospheres occurred by adding dithiothreitol as a reducing agent. As a result, glutathione was released while maintaining the nanosphere structure, and the guest molecules were gradually released.[90] Thus, it was shown that TG is useful as a drug carrier responding to a reducing environment.

We also synthesised a novel trigonal glutathione conjugate having a 1,3,5-tris(aminomethyl)-2,4,6-triethylbenzene core (Figure 5B).[91] Three glutathione units were regulated to orient toward the same side of a benzene ring due to the alternative conformation of the core. The conformation-regulated trigonal glutathione self-assembled into hard spherical structures with sizes of (310 ± 50) nm (Figure 4B), which had regular morphologies and enhanced rigidities compared to particles formed from conformationally non-regulated trigonal glutathione.

Another example of a trigonal conjugate bearing short peptides was reported by Gazit and co-workers,[92] who designed a trigonal conjugate of di-tryptophan (WW) having a tertiary amine core inspired by the clathrin triskelion. The trigonal-WW conjugate self-assembled into nanospheres with diameters of 200–500 nm in a 60% methanol/water mixture. In contrast, a conjugate containing an FF dipeptide connected to the tertiary amine scaffold afforded the formation of nanotubes with the sporadic appearance of vesicular structures, indicating that the WW dipeptide is a critical core motif, which is essential for the formation of nanospheres.

3-3. Trigonal coiled-coil-forming peptide assemblies

A coiled-coil structure is a super secondary structure consisting of a bundle of right-handed α-helixes frequently found in natural proteins, which are also important structural motifs for constructing peptide self-assemblies.[93] A coiled-coil structure can be designed by choosing the proper arrangement of hydrophobic, electrostatic and hydrogen bonding amino acid residues on the helical wheel. Arai and co-workers demonstrated that a dimeric 4-helix bundle coiled-coil structure bearing a trimeric foldon domain self-assembled into a 6-mer barrel, a 12-mer tetrahedron, an 18-mer triangle pole and a 24-mer cube.[94] Jerala and co-workers developed a novel strategy, named 'peptide origami', for constructing discrete tetrahedral objects with a 5 nm edge from single polypeptide chains composed of 12 concatenated coiled-coil-forming segments.[95-97] Robinson and co-workers demonstrated that coiled-coil-forming peptides bearing lipid tails self-assembled into viral capsid-like particles with a size of about 20 nm (Figure 6A).[98] They also showed that multiple copies of a peptide antigen, such as the V3 region of gp120 from HIV-1, can be displayed on these particles —and that they can be used for the adjuvant free stimulation of antigen-specific humoral immune responses. Ryadnov and co-workers designed a coiled-coil dimer with a disulfide bond to self-assemble into dendrimeric viral capsid-like shells with a size of 20 nm.[99] These shells were able to encapsulate DNA and siRNA and transfer them into human cells.

The trigonal conjugation of coiled-coil-forming peptides facilitates the self-assembly into spherical structures, similar to the case of trigonal β-sheet-forming peptides. For example, Woolfson and co-workers demonstrated that two complementary trigonal hubs composed of coiled-coil bundles (Hub A and Hub B) co-assembled into unilamellar spheres with a size of (97 ± 19) nm (Figure 6B).[100] AFM images of the peptide cage on a mica substrate showed flattened discs, (9.2 ± 1.0) nm thick, which indicates that the peptide cages are hollow and unilamellar. Recently, Ryadnov and co-workers developed a trigonal conjugate of K-β-Ala-K-β-Ala hub bearing three antimicrobial peptides with positive charges [C_3 (+) strand], which selectively formed a coiled-coil structure together with a complementary antagonist peptide with negative charges [C_1 (–) strand] (Figure 6C).[101] The C_1(–) strand has a Cys cap at the N-terminus, which acts as a proximal cross-linker for the

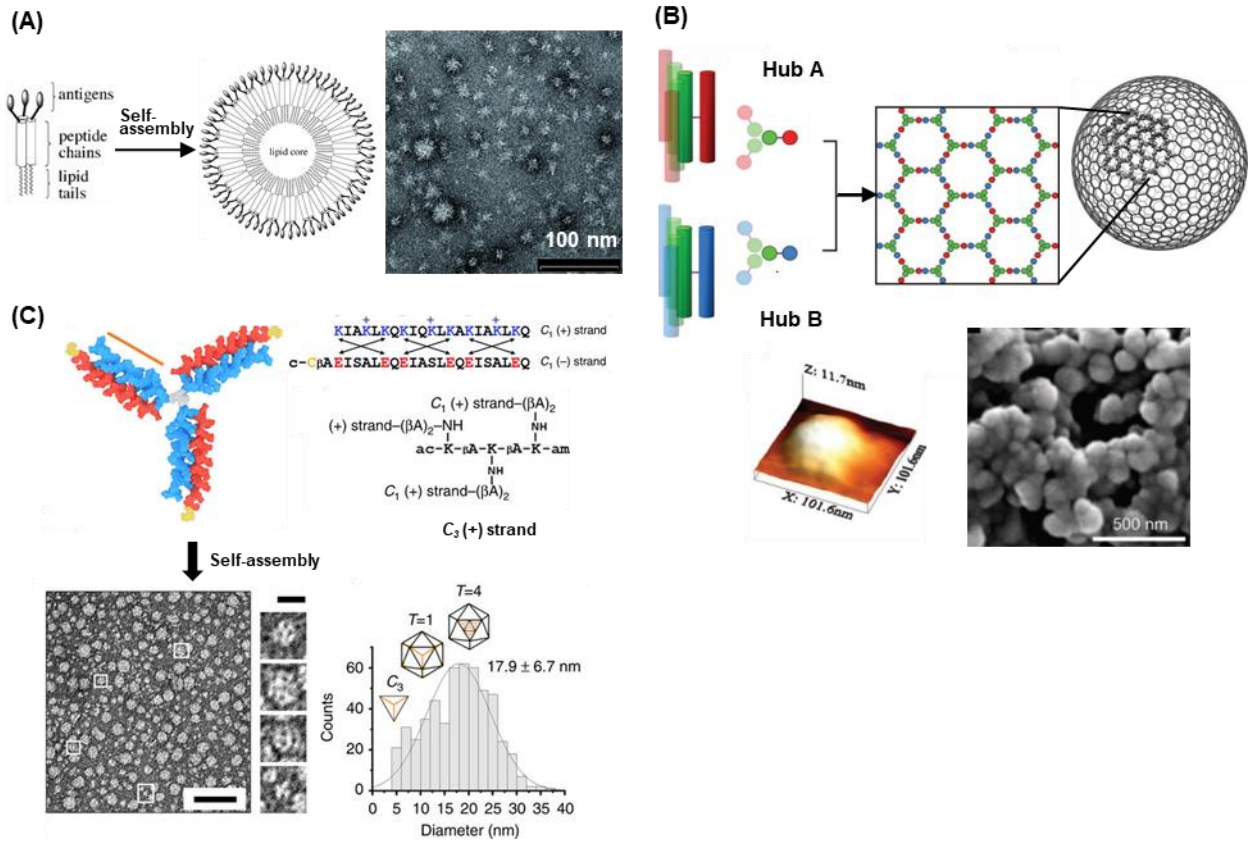

Fig. 6 Peptide nanospheres self-assembled from coiled-coil-forming peptides. (A) Coiled-coil-forming peptides bearing lipid tails and antigens developed by Robinson et al. (Reproduced with permission from ref. 98. Copyright 2007, John Wiley and Sons). (B) Complementary trigonal hubs composed of coiled-coil bundles (Hub A and Hub B) to form a spherical cage developed by Woolfson et al. (Reproduced with permission from ref. 100. Copyright 2013, American Association for the Advancement of Science). (C) Trigonal conjugates of coiled-coil-forming antimicrobial peptides [C_3 (+) strand] and the complementary antagonist peptide [C_1 (-) strand] developed by Ryadnov et al. (Reproduced with permission from ref. 101).

peptides and induces hydrophobic clustering. High-resolution TEM images of a C_3 (+) strand (100 μM) assembled with a C_1 (–) strand at a 1:3 molar ratio showed broadly spherical assemblies with an average diameter of (17.9 ± 6.7) nm. This diameter is comparable to the expected diameter (~20 nm) for a model icosahedral assembly with T = 4. Cryo-TEM and tomography analyses of the capsid-like assemblies revealed hollow shells having diameters of 20–24 nm. The capsid-like assemblies consisting of a C_3 (+) strand showed a strongly antimicrobial activity with no apparent haemolytic behaviour at micromolar concentrations. High-speed AFM imaging revealed that the capsid-like assemblies attack bacterial membranes and upon landing on phospholipid bilayers, they instantaneously convert into rapidly expanding pores, causing membrane lysis. Thus, the designed capsids destroy bacteria on contact.

As stated above, the number of examples of the construction of viral capsid-like nanospheres based on trigonal arrangements of self-assembling peptides is constantly increasing, and this procedure has now been accepted as a general method for molecular design.

4. Viral capsid-like nanocapsules self-assembled from viral β-annulus peptides

4-1. Self-assembly of β-annulus peptide from TBSV

Although the self-assembly of trigonal peptide conjugates affords nanospheres, it is difficult to selectively modify the surface and interior of these structures. If viral capsid-like nanocapsules can be constructed from peptide fragments containing subunits of viral capsids, such peptide fragments would be promising candidates as components of 'chemically designable artificial viral capsids'. Many spherical viruses, such as the sesbania mosaic virus,[102] the desmodium yellow mottle tymovirus,[103] the ryegrass mottle virus,[104] the cucumber necrosis virus,[105] the tobacco necrosis virus,[106] the turnip yellow mosaic virus,[107] and the TBSV[7, 8] have a 'β–annulus motif', which is a trimeric annular β-structure. The TBSV capsid is formed by the self-assembly of 180 quasi-equivalent protein subunits containing 388 amino acids in which the β-annulus motif participates in the formation of a dodecahedral internal skeleton.[7, 8]

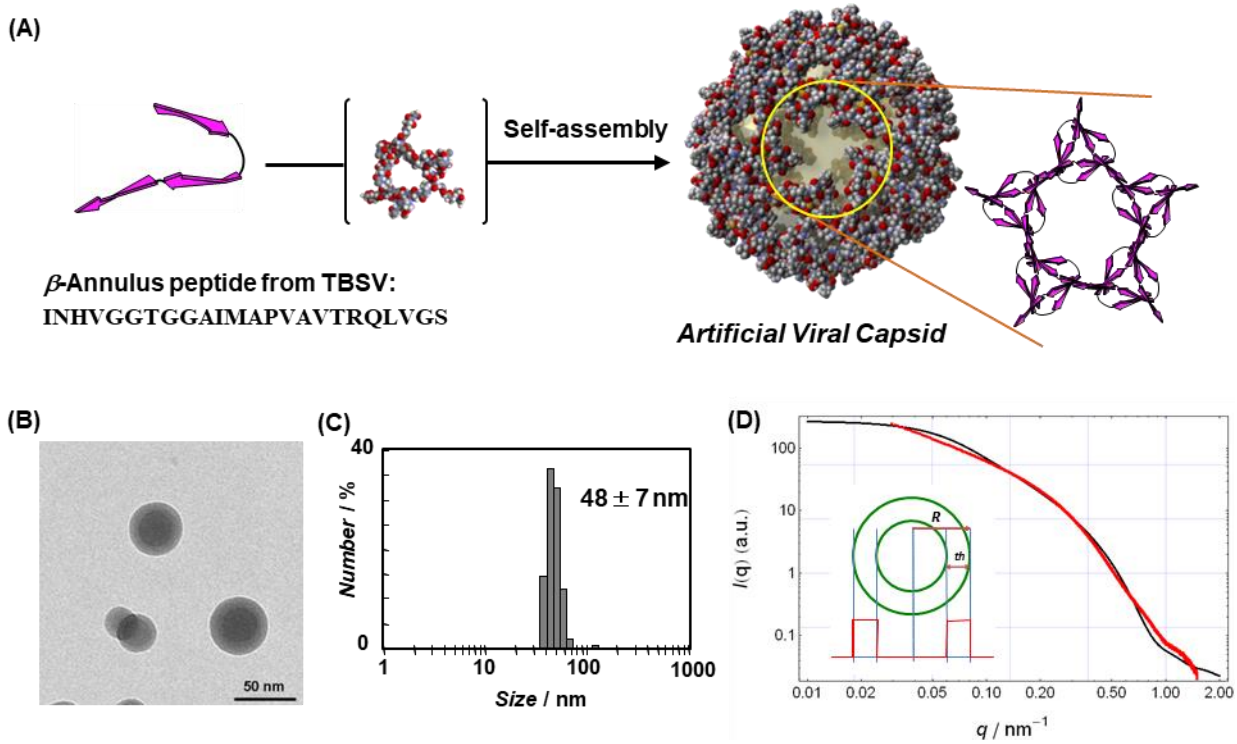

Fig. 7 Artificial viral capsids self-assembled from 24-mer β-annulus peptides from TBSV. (A) Schematic illustration of the self-assembly. (B) TEM image of the artificial viral capsids. (C) Size distribution of the artificial viral capsids, obtained from DLS experiments. (D) Synchrotron small angle X-ray scattering (SAXS) profile (red curve) of an aqueous solution of the artificial viral capsids. The black curve corresponds to the theoretical SAXS profile of a hollow capsule. Reproduced with permission from ref. 108. Copyright 2010, John Wiley and Sons.

In 2010, we found that 24-mer β-annulus peptides (INHVGGTGGAIMAPVA VTRQLVGS) of TBSV spontaneously self-assembled into hollow nanocapsules in water (Figure 7A).[108] TEM images revealed the formation of spherical assemblies (artificial viral capsids) with sizes of 30–50 nm (Figure 7B), and the average diameter, as determined by DLS, was (48 ± 7) nm in water (Figure 7C). It seems interesting that only the 24-mer β-annulus peptide fragment from TBSV formed a spherical structure without forming a unimolecular folded structure or a fibre structure. A synchrotron small angle X-ray scattering (SAXS) profile of the aqueous solution of a β-annulus peptide showed two power-law slopes: q^{-1} at the lower scattering vector region and q^{-4} at the intermediate q region, and a secondary peak at higher q regions (Figure 7D). The SAXS profile was fitted well to a theoretical equation for a vesicle model with a radius of gyration of (25 ± 11.2) nm and a wall thickness of (7.0 ± 1.4) nm, indicating the existence of a cavity inside the artificial viral capsid. The critical aggregation concentration (CAC) of the β-annulus peptide was determined from the concentration dependence of the DLS count rate and was found to be 25 μM in water at 25°C. The size and morphology of the artificial viral capsid were minimally affected at concentrations above CAC, indicating that spherical assemblies with sizes of about 30–50 nm are thermodynamically stable. We also demonstrated that the β-annulus peptide of a sesbania mosaic virus bearing an FKFE sequence at the C-terminus self-assembled into nanospheres with a size of about 30 nm in an acidic aqueous solution.[109]

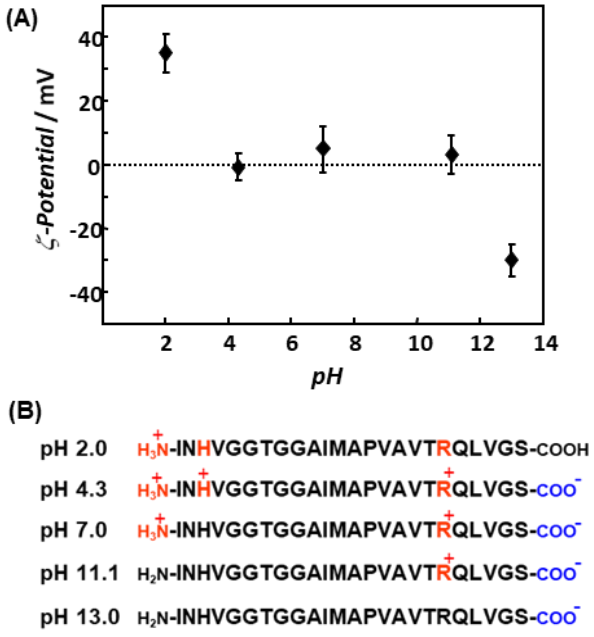

Fig. 8 (A) Effect of the pH on the the ζ-potentials of artificial viral capsids self-assembled from β-annulus peptides. (B) Expected charges on β-annulus peptides at various pH values. Reproduced with permission from ref. 110. Copyright 2013, Springer Nature.

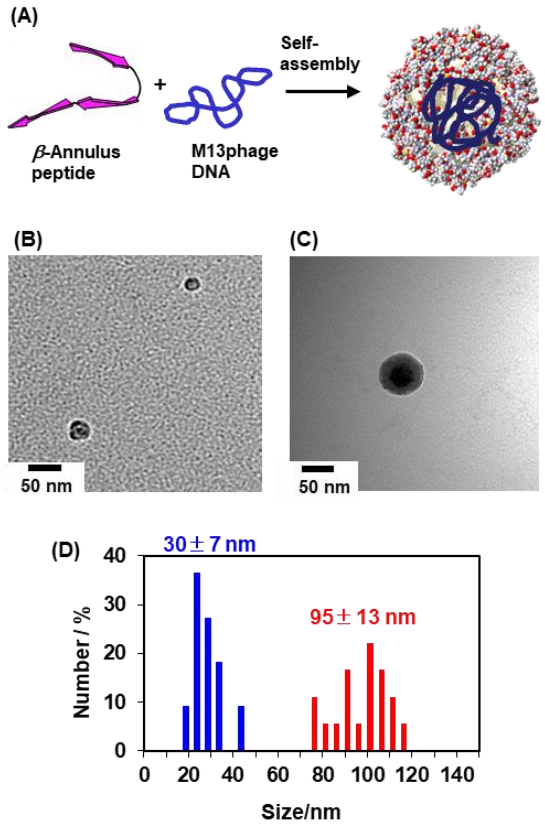

Fig. 9 (A) Schematic representation of the encapsulation of M13 phage DNA into the cationic interior of artificial viral capsids self-assembled from *β*-annulus peptides. (B, C) TEM images of aqueous solutions of *β*-annulus peptides in the presence of M13 phage DNA stained with cisplatin (B) and with cisplatin followed by uranyl acetate (C). (D) Size distribution obtained from TEM images stained with cisplatin (red) and cisplatin + uranyl acetate (blue). Reproduced with permission from ref. 110. Copyright 2013, Springer Nature.

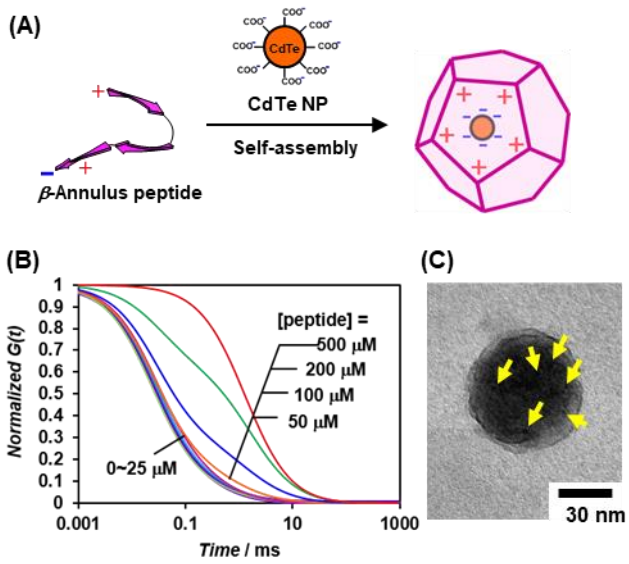

Fig. 10 (A) Schematic illustration of the encapsulation of CdTe quantum dots into the cationic interior of artificial viral capsids self-assembled from *β*-annulus peptides. (B) Normalized autocorrelation curves of a mixture of CdTe NPs (0.1 μM) and *β*–annulus peptides at 0–500 μM, obtained from fluorescence correlation spectroscopy (FCS). (C) TEM image of CdTe NP-encapsulated artificial viral capsids stained with ruthenium tetroxide. The arrows show the positions of the CdTe NPs. Reproduced with permission from ref. 111. Copyright 2016, Chemical Society of Japan.

4-2. Encapsulation into artificial viral capsids

Although natural TBSV capsids encapsulate RNA, artificial viral capsids self-assembled from *β*-annulus peptides of TBSV are expected to encapsulate various guest molecules in their hollow interior. To investigate the surface charge on the artificial viral capsids, we measured the pH dependence of the *ζ*-potential (Figure 8).[110] The results indicate that the surface *ζ*-potentials of the artificial viral capsids are dominated by the charges of the C-terminal sequence (RQLVGS-COOH), and that the N-terminal sequence (H_2N-INH) has a minimal effect. Our observations suggest that the C-terminal is directed to the outer surface, whereas the N-terminal is directed to the interior of the artificial capsids, which corresponds to the terminal-direction of the natural TBSV capsid. Thus, the interior of the peptide nanocapsules should be cationic at pH 7. Actually, the artificial viral capsids tended to encapsulate anionic dyes rather than cationic dyes.

Polyanionic M13 phage DNA was also encapsulated in the artificial viral capsids (Figure 9A).[110] An aqueous solution of *β*-annulus peptide was gradually added to an aqueous solution of M13 phage DNA at pH 4.3 to produce equimolar complexes of the cation and the anion. The DNA/*β*-annulus peptide complexes did not precipitate, and their average size was estimated (by DLS) to be (82 ± 17) nm. TEM observations of complexes stained with cisplatin, which selectively binds to DNA, showed the formation of globular DNA particles with a diameter of (30±7) nm (Figure 9B, D), whereas in the absence of *β*-annulus peptides, DNA molecules with irregular morphology were observed by TEM. When an uranyl acetate stain was added to DNA/peptide 1 complexes previously stained with cisplatin, core-shell nanospheres with a diameter of (95 ± 13) nm were observed by TEM (Figure 9C, D). These results indicate that the M13 phage DNA was compacted and encapsulated in the artificial viral capsids to form core-shell spheres. This dynamic transformation into core-shell nanospheres is one of the most important features of the present *β*-annulus peptide assemblies. This behaviour is consistent with the proposed dynamic equilibrium of *β*-annulus peptide assemblies, which allows them to re-organise upon the binding of guest molecules.

An *in situ* analysis of the encapsulation behaviour of anionic CdTe quantum dots (3 nm) into artificial viral capsids was performed by using fluorescence correlation spectroscopy (FCS) (Figure 10A),[111] which is a technique in which spontaneous fluorescence intensity fluctuations are measured in a microscopic detection volume. The autocorrelation function (*G(t)*) of the aqueous dispersion of CdTe nanoparticles alone

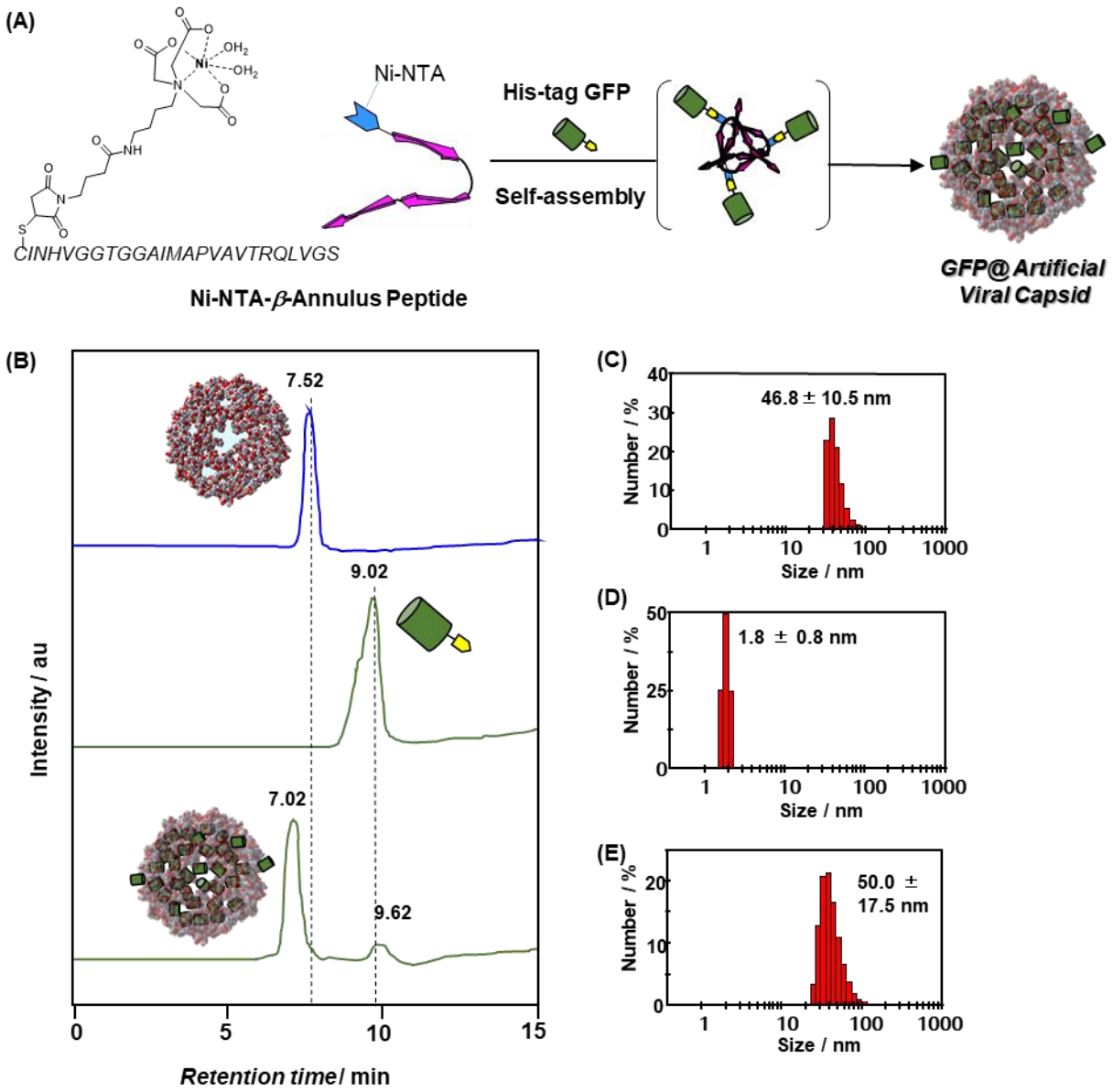

Fig. 11 (A) Schematic illustration of encapsulation of His-tagged GFP into the artificial viral capsids self-assembled from Ni-NTA-modified β-annulus peptide. (B) Size exclusion chromatograph of the artificial viral capsids (upper), His-tagged GFP (middle), and equimolar mixture of His-tagged GFP and Ni-NTA-modified β-annulus peptide (lower). (C-E) Size distributions obtained from DLS of the artificial viral capsids (C), His-tagged GFP (D), and equimolar mixture of His-tagged GFP and Ni-NTA-modified β-annulus peptide (E). Reproduced with permission from ref. 112. Copyright 2016, Royal Society of Chemistry.

showed a simple sigmoidal decay curve, which was fitted well to the theoretical equation for a single-component model. In contrast, the autocorrelation function of CdTe nanoparticles in the presence of 50–200 μM β-annulus peptide showed a two-step decay curve, which was fitted to the dual-component model, indicating the co-existence of fast and slow components (Figure 10B). At 500 μM, the autocorrelation function curve was fitted to a single-component model comprising only a slow component. The apparent hydrodynamic diameters were calculated using the Stokes–Einstein equation and the diffusion time of the CdTe nanoparticles was determined by FCS curve fitting. The apparent diameter of the fast component was estimated to be about 3 nm, which corresponds to the diameter of CdTe nanoparticles, whereas the diameter of the slow component appeared at β-annulus peptide concentrations of 50–500 μM and were estimated to be about 30–50 nm, which is similar to the diameter of artificial viral capsids. These results indicate that CdTe nanoparticles were encapsulated into the artificial viral capsids at concentrations above 50 μM, which corresponds to the CAC of the β-annulus peptide (25 μM). A TEM image of CdTe nanoparticles in the presence of β-annulus peptides (stained with RuO_4) showed that many CdTe nanoparticles overlapped with the peptide assemblies, and that almost no nanoparticles were observed outside the capsid (Figure 10C), suggesting that most nanoparticles were encapsulated.

Since —as mentioned above— the N-terminals of β-annulus peptides are directed toward the interior, the N-terminal modification of these peptides could enable selective encapsulation within artificial viral capsids. To encapsulate His-tagged proteins into artificial viral capsids, β-annulus peptides modified with Ni-NTA (nitrilotriacetic acid) at the N-terminal were synthesised (Figure 11A).[112] The Ni-NTA-modified β-annulus peptide self-assembled into artificial viral capsids with a size of (46.8 ± 10.5) nm (Figure 11C), which is comparable to the diameter of artificial viral capsids self-assembled from unmodified 24-mer β-annulus peptides. The concentration dependence of Ni-NTA-modified β-annulus peptide scattering intensities indicated that the CAC at 25°C is 0.053 μM, which is 470 times lower than the CAC of unmodified β-annulus peptides under the same conditions. Size exclusion chromatography (SEC) studies of Ni-NTA-modified β-annulus peptide assemblies and His-tagged green fluorescence protein (His-tagged GFP) alone showed single elution peaks at 7.52 and 9.02 min, respectively. SEC experiments of equimolar mixtures of His-tagged GFP and the Ni-NTA-modified peptide assembly showed two elution peaks at 7.02 and 9.62 min (Figure 11B), reflecting 91% encapsulation of GFP in the artificial viral capsids and 9% free GFP, respectively. A DLS study of equimolar mixtures of His-tagged GFP and the Ni-NTA-modified peptide assembly gave average diameters of (50.0 ± 17.5) nm (Figure 11E), suggesting that encapsulation of His-tagged GFP had only a minimal effect on the size distribution.

Similarly, fluorescent ZnO nanoparticles (10 nm) were encapsulated in artificial viral capsids self-assembled from β-annulus peptides bearing a ZnO-binding sequence (HCVAHR) at the N-terminal.[113] DLS experiments showed that in the presence of the peptide, the ZnO nanoparticles formed assemblies with an average size of (48 ± 24) nm, whereas in the absence of the peptide the nanoparticles formed large aggregates. The fluorescence spectrum of ZnO nanoparticles in the presence of ZnO-binding β-annulus peptide exhibited an enhanced emission peak at 410 nm, which is ascribed to the electronic passivation effect caused by the interaction between the ZnO-binding peptide and the ZnO surface encapsulated in the artificial viral capsid. We envisage that the artificial viral capsid can encapsulate various inorganic materials, biomacromolecules and synthetic polymers through proper modification of their interior.

4-3. Surface decoration of artificial viral capsids

As described above, it was suggested that the C-terminals of β-annulus peptides are directed toward the outer surface of artificial viral capsids. Thus, it is possible to create artificial viral capsids decorated with functional molecules at the outer surface by proper modification of the C-terminals of the β-annulus peptide. For example, artificial viral capsids decorated with gold nanoparticles (AuNPs) can be constructed by self-assembly of β-annulus peptides modified with AuNP at the C-terminal (Figure 12A).[114] An AuNP–β-annulus peptide conjugate was prepared by mixing Cys-containing β-annulus peptide at the C-terminal with AuNPs at a concentration below the CAC,

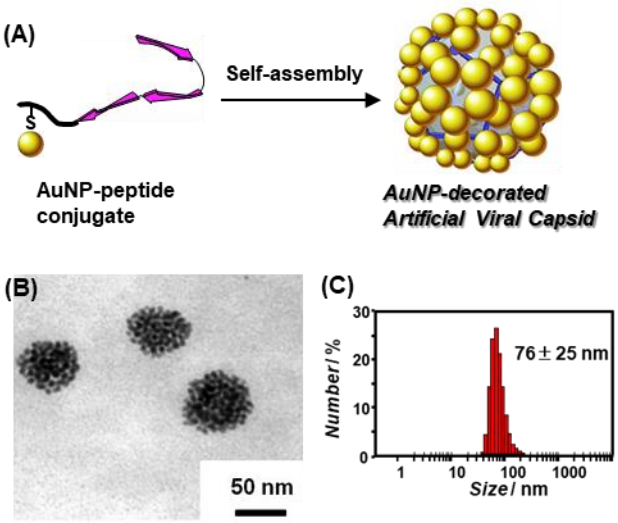

Fig. 12 Gold nanoparticles (AuNPs)-decorated artificial viral capsids. (A) Schematic illustration of the self-assembly. (B) TEM image. (C) Size distribution obtained from DLS. Reproduced with permission from ref. 114. Copyright 2014, Springer Nature.

followed by protection with thioctic acid. After concentrating to above the CAC, TEM images and DLS experiments showed the formation of AuNP assemblies with diameters of 30–60 nm (Figure 12B, C). The ζ-potential of the AuNP assemblies at pH 4.6 was (−30.5 ± 9.8) mV, reflecting charges of thioctic acid on the AuNPs, whereas that of unmodified artificial viral capsids at the same pH was (0.01 ± 9.8) mV. These results indicate that AuNPs decorated the outer surface of the artificial viral capsids.

Single-strand DNA-decorated artificial viral capsids can also be constructed by self-assembly of β-annulus peptides connected to DNA at the C-terminal (Figure 13A).[115] DNA-conjugated β-annulus peptides were prepared by the reaction of Cys of β-annulus peptides at the C-terminal with maleimide-modified DNAs (dA_{20} and dT_{20}). The dA_{20}-conjugated β-annulus peptides self-assembled into artificial viral capsids with sizes of 45–160 nm, despite anionic repulsion (Figure 13B, C). When complementary polynucleotides (poly-dT) were added to the dA_{20}-decorated artificial viral capsids, aggregates were formed (Figure 13D, E). In contrast, such aggregation was minimally observed in an equimolar mixture of dA_{20}-conjugated β-annulus peptides and non-complementary Poly-dA (Figure 13F, G). These results indicate that DNA displayed on the surface of an artificial viral capsid can recognise the complementary DNA, which induces aggregation of the DNA-coated capsids by crosslinking among capsids with polynucleotide chains.

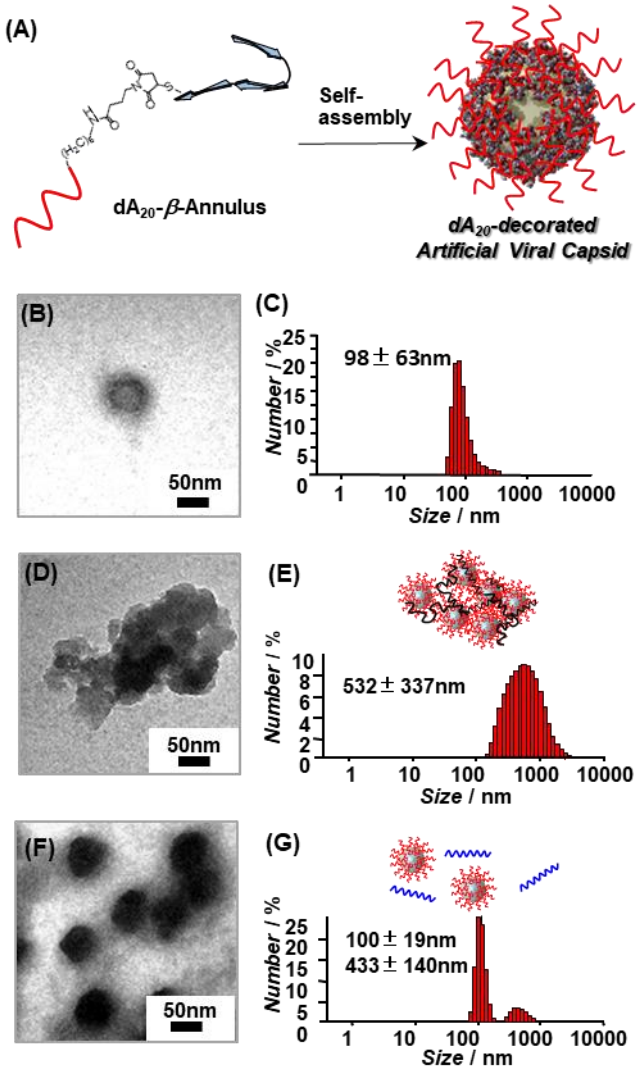

Fig. 13 (A) Schematic illustration of formation of DNA-decorated artificial viral capsids. (B, C) TEM image and size distribution obtained from DLS of dA_{20}-decorated artificial viral capsids. (D-G) TEM images and size distributions obtained from DLS of dA_{20}-decorated artificial viral capsids in the presence of poly-T (D, E) and in the presence of poly-dA (F, G). Reproduced with permission from ref. 115. Copyright 2017, John Wiley and Sons.

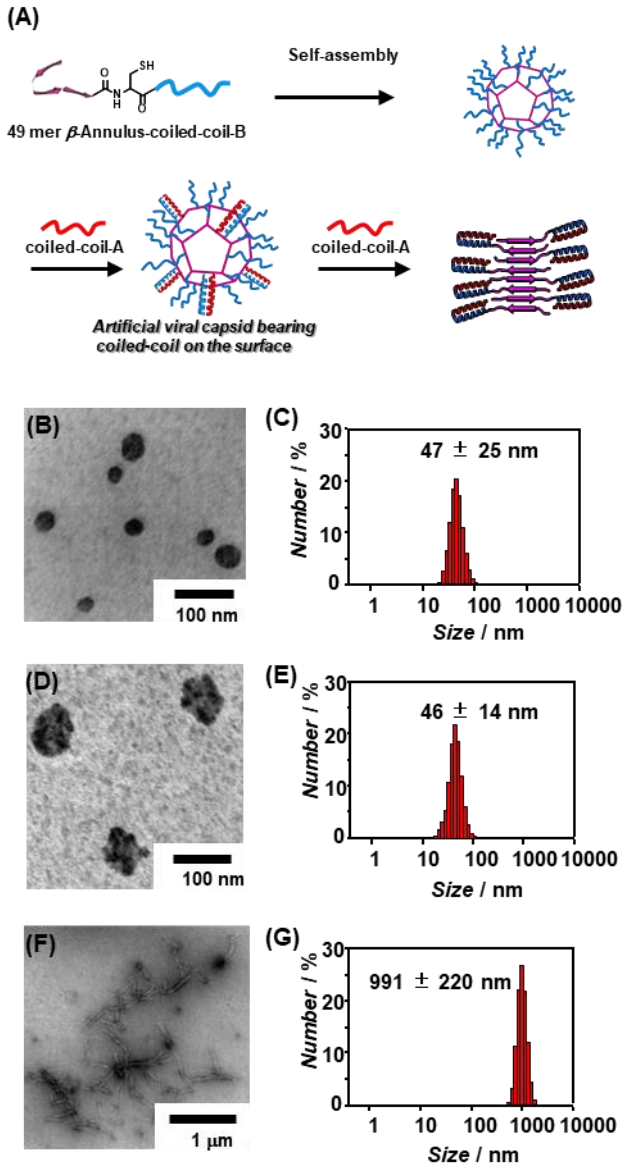

Fig. 14 (A) Schematic illustration of the formation of artificial viral capsids bearing coiled-coils at the surface and fibrous assemblies. (B, C) TEM image and size distribution obtained from DLS experiments of an aqueous solution of β-annulus-coiled-coil-B peptides. (D-G) TEM images and size distributions obtained from DLS measurements on 4:1 (D, E) and 1:1 mixtures (F, G) of β–annulus-coiled-coil-B peptide and coiled-coil-A. Reproduced with permission from ref. 116. Copyright 2017, Royal Society of Chemistry.

Some natural viruses, such as adenovirus and influenza virus, have protein spikes on their surface, and it is known that the spikes on the viral capsid increase cell-surface recognition and infectivity owing to the increased surface area. To construct artificial viral capsids bearing protein spikes, we designed a complementary dimeric coiled-coil-forming β-annulus peptide (Figure 14A).[116] A β-annulus peptide bearing a coiled-coil-forming sequence at the C-terminus (β-annulus-coiled-coil-B) was synthesised by a native chemical ligation of β-annulus-SBn peptide with Cys-containing coiled-coil-B peptide. The peptide self-assembled into an artificial viral capsid with a size of about 50 nm (Figure 14B, C). CD spectra showed the formation of coiled-coils with the addition of complementary coiled-coil-A peptide to the coiled-coil-B-displayed artificial viral capsid. A DLS study of the 4:1 mixture of β-annulus-coiled-coil-B peptide and coiled-coil-A peptide showed the formation of assemblies with a size of (46 ± 14) nm (Figure 14E), which is comparable to the size of an artificial viral capsid self-assembled from β-annulus-coiled-coil-B peptide alone (Figure 13C). A TEM image of the 4:1 mixture showed the formation of spherical assemblies with a size of 60 nm bearing grains of about 5 nm on the surface (Figure 14D). We believe that these grains could be ascribed to dimeric coiled-coil spikes. In contrast, the TEM image of the 1:1 mixture indicated the formation of fibrous assemblies with a length of about 1 μm (Figure 14F), which is

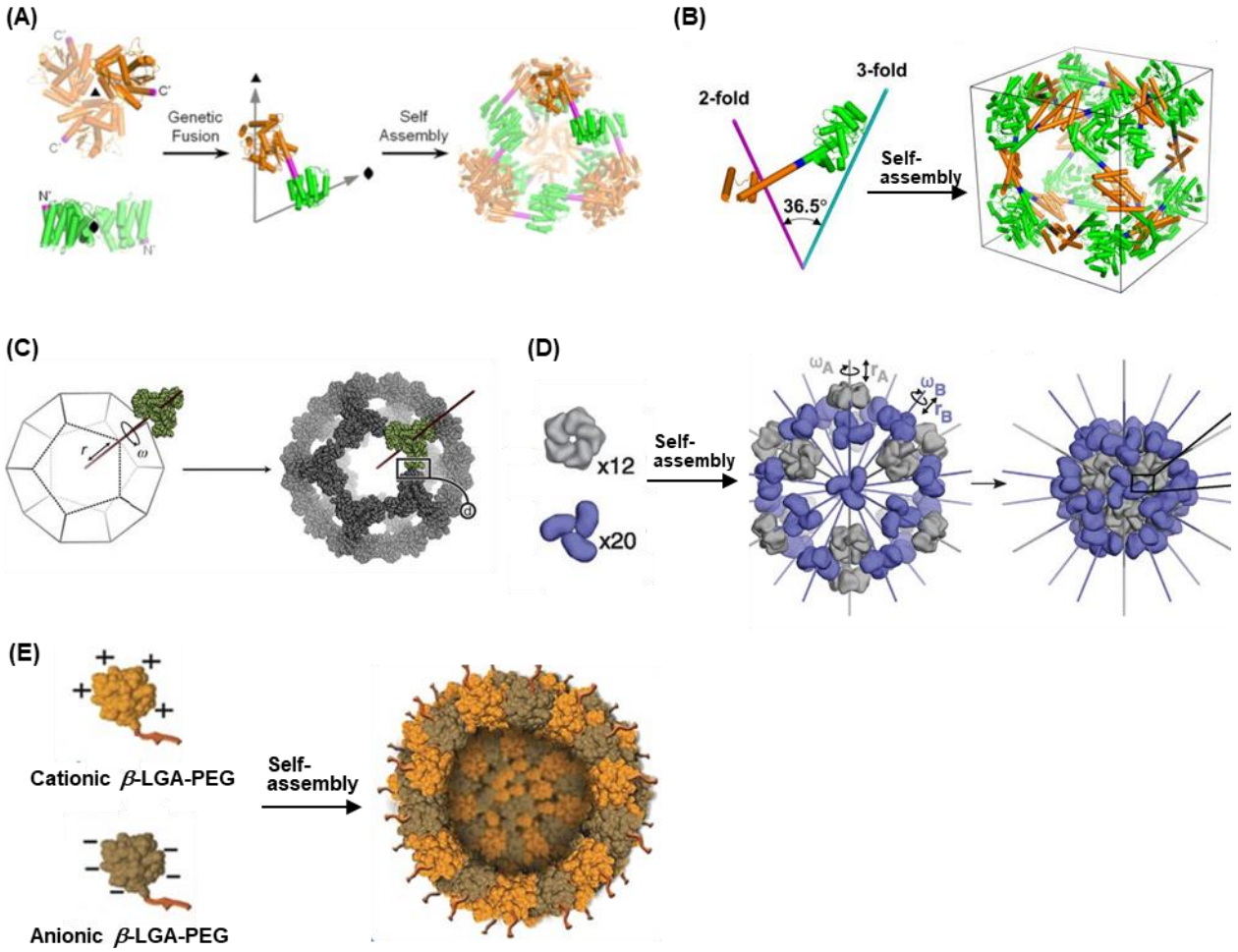

Fig. 15 Viral capsid-like nanocapsules self-assembled from rationally designed proteins. (A) Tetrahedral protein cage developed by Yeates et al. (Reproduced with permission from ref. 119, Copyright 2013, American Chemical Society). (B) Cubic protein cage developed by Yeates et al. (Reproduced with permission from ref. 120. Copyright 2014, Springer Nature). (C) Icosahedral protein cage self-assembled from trimeric protein building blocks developed by Baker et al. (Reproduced with permission from ref. 121. Copyright 2016, Springer Nature). (D) Icosahedral protein cage co-assembled from pentameric and trimeric protein building blocks developed by Baker et al. (Reproduced with permission from ref. 122, Copyright 2016, American Association for the Advancement of Science). (E) Protein nanocapsule self-assembled from cationic and anionic β-lactoglobulin A-PEG conjugates developed by Nallani et al. (Reproduced with permission from ref. 123, Copyright 2017, John Wiley and Sons).

supported by the size distribution obtained from DLS measurements (Figure 14G).

As described above, artificial viral capsids decorated with AuNPs, DNA and coiled-coil peptides have been developed. We envisage that the present strategy for surface decoration of artificial viral capsids could be extended to the creation of functional artificial viral capsids modified with various biomacromolecules such as enzymes, receptor proteins, antigens and so on.

5. Viral capsid-like nanocapsules self-assembled from designed proteins

Another approach to constructing viral capsid-like nanocapsules involves the use of rationally designed proteins. In 2001, a pioneering work on the construction of three-dimensional protein cage assemblies was reported by Yeates and co-workers,[117, 118] who revealed that a fusion protein consisting of a trimer-forming unit (bromoperoxidase) and a dimer-forming unit (M1 matrix protein of the influenza virus) connected by a helical linker self-assembled into 16-nm tetrahedral protein cages (Figure 15A).[119] The researchers also succeeded in constructing 22.5-nm cubic structures by self-assembly of a fusion protein of KDPG aldolase as the trimer-forming unit with FkpA protein as the dimer-forming unit (Figure 15B).[120]

Recently, Baker and co-workers demonstrated the computational design of a 25-nm icosahedral nanocage that self-assembles from trimeric protein building blocks (Figure 15C).[121] Cryo-TEM experiments showed that the designed protein (I3-01) self-assembled into a homogenous population of icosahedral particles nearly identical to the design model. Interestingly, the I3-01 protein cages were very stable to denaturation and heat (up to 80ºC). The fusion protein

consisting of I3-01 and superfolder GFP (I3-01-sfGFP) self-assembled into a GFP-decorated icosahedral protein cage, which functions as a highly fluorescent 'standard candle' for use in light microscopy. Moreover, the researchers designed co-assembling, two-component proteins, which assembled into 120-subunit icosahedral protein nanostructures with diameters of 24–40 nm.[122] For example, an I53 architecture is formed from the combination of 12 pentameric building blocks and 20 trimeric building blocks aligned along the fivefold and threefold icosahedral symmetry axes, respectively (Figure 15D). TEM and SAXS investigations revealed that the designed proteins form icosahedral cages closely matching the computational design models. Supercharged GFP (net charge: -30) can be encapsulated into icosahedral protein cages having a cationic interior through charge complementarity.

A simple approach for constructing protein nanocapsules was demonstrated by Nallani and co-workers (Figure 15E),[123] who synthesised conjugates composed of β-lactoglobulin A and poly(ethylene glycol) with a negative [βLGA-PEG (−)] and a positive [βLGA-PEG (+)] supercharge, respectively. An equimolar mixture of oppositely charged βLGA-PEG conjugates self-assembled into spherical protein capsules with diameters of 80–100 nm. Guest molecules such as GFP and fluorescein isothiocyanate (FITC)–dextran were encapsulated into the protein nanocapsules without influencing the self-assembly. It is expected that this simple approach to construct nanocapsules would be applicable to other globular proteins.

Conclusions and perspective

This review article discussed recent advances in molecular design for the construction of viral capsid-like spherical nanoassemblies. Trigonal conjugation of self-assembling peptides, such as β-sheet-forming peptides, glutathione and coiled-coil-forming peptides, is becoming a general strategy to construct viral capsid-like nanoparticles. β-Annulus peptides, which are viral peptide fragments participating in the formation of internal skeletons, are also useful for self-assembling units to construct viral capsid-like nanocapsules. More precise viral capsid-like nanocapsules have been constructed by self-assembly of rationally designed fusion proteins bearing symmetric assembling units.

The advantages of peptide-based viral capsid-like nanocapsules include diverse molecular designs and the ease for syntheses, but the relatively broad size distribution should still be overcome. A dynamic equilibrium in the self-assembly of peptide-based viral capsid-like nanocapsules facilitates encapsulation and release of guest molecules such as drugs, proteins and nucleic acids. Also, various functionalities including cell-targeting ability, releasing ability of included materials, catalytic ability, stimuli-responding ability and immunogenicity can easily be introduced into the peptide-based viral capsid-like nanocapsules, and these functionalised artificial viral capsids could then be applied as drug carriers, vaccine platforms, nanotemplates and nanoreactors. Understanding the assembly/disassembly mechanism of viral capsid-like nanocapsules by thermodynamic and kinetic analysis is important issue for the applications.[124-126] Comparison of assembly/disassembly mechanism of between natural and artificial viral capsids would provide novel design strategy for synthetic viral capsid-like nanocapsules.

Future targets for the investigation of artificial viral capsids include the development of envelop-type[127, 128] and self-replicating artificial viruses as well as the analysis of the self-assembly process under molecular crowding conditions.[129] Another interesting feature of natural viral capsids is post-modification of viral capsids during the replication cycle to change the morphology of their capsids or reinforce their capsids. Development of artificial viral capsids having such evolutional feature is also included in next target. We believe that these synthetic-chemistry-based viral capsid-like materials could open up new areas of research in supramolecular chemistry, peptide chemistry, protein engineering, medicinal chemistry and nanotechnology.

Conflicts of interest

There are no conflicts to declare.

Acknowledgements

I would like to thank Prof. Nobuo Kimizuka (Kyushu University) and all the colleagues whose names are cited in the references for their valuable contributions. This work was partially supported by PRESTO, Japan Science and Technology Agency (JST) and KAKENHI (No.15H03838, 18H02089 and 18H04558) from the Japan Society for the Promotion of Science (JSPS).

Notes and references

1 *Viruses: Biology, Applications, and Control*, D. R. Harper, Garland Science, Taylor & Francis Group, 2012.
2 *Structure and Physics of Viruses*, M. G. Mateu (Ed.), Springer, 2013.
3 J. E. Johnson and J. A. Speir, *J. Mol. Biol*., 1997, **269**, 665.
4 B.V. V. Prasad and M. F. Schmid, *Adv Exp Med Biol.*, 2012, **726**, 17.
5 M. G. Mateu, *Arch. Biochem. Biophys.*, 2013, **531**, 65.
6 P. Plevka, S. Hafenstein, P. Tattersall, S. Cotmore, G. Farr, A. D'Abramo, and M. G. Rossmann, *J. Virol*., 2011, **85**, 4822.
7 A. J. Olson, G. Bricogne and S. C. Harrison, *J. Mol. Biol.*, 1983, **171**, 61.
8 P. Hopper, S. C. Harrison, R. T. Sauer, *J. Mol. Biol.*, 1984, **177**, 701.
9 C. Helgstrand, S. Munshi, J. E. Johnson, and L. Liljas, *Virology*, 2004, **318**, 192.
10 X. Zhang, W. Meining, M. Fischer, A. Bacher, R. Ladenstein, *J. Mol. Biol.*, 2001, **306**, 1099.
11 S. C. Harrison and T. Kirschhausen, *Cell*, 1983, **33**, 650.
12 A. Fotin, Y. Cheng, P. Sliz, N. Grigorieff, S. C. Harrison, T. Kirchhausen and T. Walz, *Nature*, 2004, **432**, 573.
13 C. Uetrecht, I. M. Barbu, G. K. Shoemaker, E. van. Duijn, A. J. R. Heck, *Nat. Chem.,* 2011, **3**, 126.
14 K. Holmes, D. A. Shepherd, A. E. Ashcroft, M. Whelan, D. J. Rowlands, N. J. Stonehouse, *J. Biol. Chem.*, 2015, **290**, 16238.
15 M. Medrano, M. A. Fuertes, A. Valbuena, P. J. P. Carrillo, A. Rodríguez-Huete, M. G. Mateu, *J. Am. Chem. Soc*., 2016, **138**, 15385.

16 C. A. Lutomski, N. A. Lyktey, Z. Zhao, E. E. Pierson, A. Zlotnick, M. F. Jarrold, *J. Am. Chem. Soc*., 2017, **139**, 16932.
17 Z. Liu, J. Qiao, Z. Niu and Q. Wang, *Chem. Soc. Rev.*, 2012, **41**, 6178.
18 Y. Ma, R. J.M. Nolte, and J. J. L. M. Cornelissen, *Adv. Drug Deliv. Rev.*, 2012, **64**, 811.
19 M. Somiya, Q. Liu, and S. Kuroda, *Nanotheranostics*, 2017, **1**, 415.
20 R. L. Garcea1 and L. Gissmann, *Curr. Opin. Biotechnol.*, 2004, **15**, 513.
21 E. M. Plummer and M. Manchester, *WIREs Nanomed. Nanobiotech.*, 2011, **3**, 174.
22 T. Douglas and M. Young, *Nature*, 1998, **393**, 152.
23 T. Douglas and M. Young, *Science*, 2006, **312**, 873.
24 M. Uchida, M. T. Klem, M. Allen, P. Suci, M. Flenniken, E. Gillitzer, Z. Varpness, L. O. Liepold, T. Douglas, and M. Young, *Adv. Mater.*, 2007, **19**, 1025.
25 N. F. Steinmetz and D. J. Evans, *Org. Biomol. Chem.*, 2007, **5**, 2891.
26 L. M. Bronstein, *Small*, 2011, **7**, 1609.
27 L. S. Witus and M. B. Francis, *Acc. Chem. Res.*, 2011, **44**, 774.
28 A. M. Wen and N. F. Steinmetz, *Chem. Soc. Rev.*, 2016, **45**, 4074.
29 T. Douglas, E. Strable, D. Willits, A. Aitouchen, M. Libera, M. Young, *Adv. Mater.*, 2002, **14**, 415.
30 C. Chen, M. C. Daniel, Z. T. Quinkert, M. De, B. Stein, V. D. Bowman, P. R. Chipman, V. M. Rotello, C. C. Kao, and B. Dragnea, *Nano Lett.*, 2006, **6**, 611.
31 S. K. Dixit, N. L. Goicochea, M. C. Daniel, A. Murali, L. Bronstein, M. De, B. Stein, V. M. Rotello, C. C. Kao, and B. Dragnea, *Nano Lett.*, 2006, **6**, 1993.
32 M. C. Aragonès, H. Engelkamp, V. I. Claessen, N. A. J. M. Sommerdijik, A. E. Rowan, P. C. M. Christianen, J. C. Maan, B. J. M. Verduin, J. J. L. M. Cornelissen, R. J. M. Nolte, *Nature Nanotech.*, 2007, **2**, 635.
33 D. P. Patterson, P. E. Prevelige, and T. Douglas, *ACS Nano*, 2012, **6**, 5000.
34 D. P. Patterson, B. Schwarz, R. S. Waters, T. Gedeon, and T. Douglas, *ACS Chem. Biol.*, 2014, **9**, 359.
35 M. Brasch, R. M. Putri, M. V. de Ruiter, D. Luque, M.. S. T. Koay, J. R. Castón, and J. J. L. M. Cornelissen, *J. Am. Chem. Soc.*, 2017, **139**, 1512.
36 Y. Azuma, R. Zschoche, M. Tinzl, D. Hilvert, *Angew. Chem. Int. Ed.*, 2016, **55**, 1531.
37 F. P. Seebeck, K. J. Woycechowsky, W. Zhuang, J. P. Rabe, and D. Hilvert, *J. Am. Chem. Soc.*, 2006, **128**, 4516.
38 B. Wörsdörfer, Z. Pianowski, and D. Hilvert, *J. Am. Chem. Soc.*, 2012, **134**, 909.
39 I. J. Minten, L. J. A. Hendriks, R. J. M. Nolte and J. J. L. M. Cornelissen, *J. Am. Chem. Soc.*, 2009, **131**, 17771.
40 A. O'Neil, P. E. Prevelige, G. Basu, and T. Douglas, *Biomacromolecules*, 2012, **13**, 3902.
41 J.-K. Rhee, M. Hovlid, J. D. Fiedler, S. D. Brown, F. Manzenrieder, H. Kitagishi, C. Nycholat, J. C. Paulson, and M. G. Finn, *Biomacromolecules*, 2011, **12**, 3977.
42 M. B. van Eldijk, J. C. Y. Wang, I. J. Minten, C. Li, A. Zlotnick, R. J. M. Nolte, J. J. L. M. Cornelissen, J. C. M. van Hest, *J. Am. Chem. Soc.*, 2012, **134**, 18506.
43 A. S. Blum, C. M. Soto, C. D. Wilson, T. L. Brower, S. K. Pollack, T. L. Schull, A. Chatterji, T. Lin, J. E. Johnson, C. Amsinck, P. Franzon, R. Shashidhar, and B. R. Ratna, *Small*, 2005, **1**, 702.
44 G. J. Tong, S. C. Hsiao, Z. M. Carrico and M. B. Francis, *J. Am. Chem. Soc.*, 2009, **131**,11174.
45 N. Stephanopoulos, G. J. Tong, S. C. Hsiao, and M. B. Francis, *ACS Nano*, 2010, **4**, 6014.
46 K. S. Raja, Q.Wang, M. G. Finn, *ChemBioChem*, 2003, **4**, 1348.
47 S. S. Gupta, . S. Raja, E. Kaltgrad, E. Strable and M. G. Finn, *Chem. Commun.*, 2005, **34**, 4315.
48 A. J. Olson, Y. H. E. Hu, and E. Keinan, *Proc. Nat. Acad. Sci., USA*, 2007, **104**, 20731.
49 M. Fujita, M. Tominaga, A. Hori, and B. Therrien, *Acc. Chem. Res.*, 2005, *38*, 369.
50 D. Fujita, K. Suzuki, S. Sato, M. Yagi-Utsumi, Y. Yamaguchi, N. Mizuno, T. Kumasaka, M. Takata, M. Noda, S. Uchiyama, K. Kato, and M. Fujita, *Nat. Commun.*, 2012, **3**, 1093.
51 D. Fujita, Y. Ueda, S. Sato, H. Yokoyama, N. Mizuno, T. Kumasaka, and M. Fujita, *Chem*, 2016, **1**, 91.
52 N. C. Seeman, *Nature*, 2003, **421**, 427.
53 J. Nangreave, D. Han, Y. Liu, H. Yan, *Curr. Opin. Chem. Biol.*, 2010, **14**, 608.
54 K. Matsuura, T. Yamashita, Y. Igami, and N. Kimizuka, *Chem. Commun.*, 2003, 376.
55 K. Kim, K. Masumoto, K. Matsuura, and N. Kimizuka, *Chem. Lett.,* 2006, **35**, 486.
56 K. Matsuura, K. Masumoto, Y. Igami, T. Fujioka, and N. Kimizuka, *Biomacromolecules*, 2007, **8**, 2726.
57 K. Matsuura, K. Masumoto, Y. Igami, K. Kim, and N. Kimizuka, *Mol. BioSys.*, 2009, **5**, 921.
58 K. Kim, K. Matsuura, and N. Kimizuka, *Bioorg. Med. Chem.*, 2007, **15**, 4311.
59 W. M. Shih, J. D. Quispe, and G. F. Joyce: *Nature*, 2004, **427**, 618.
60 Y. He, T. Ye, M. Su, C. Zhang, A. E. Ribbe, W. Jiang, and C. Mao, *Nature*, 2008, **452**, 198.
61 *Peptide Materials: From Nanostuctures to Applications*, ed. C. Aleman, A. Bianco, M. Venanzi, Wiley, Weinheim, 2013.
62 Self-Assembled Peptide Nanostructures: Advances and Applications in Nanobiotechnology, ed. J. Castillo, L. Sasso, W. E. Svendsen, CRC Press, 2012.
63 K. Matsuurua, *RSC Adv.*, 2014, **4**, 2942.
64 B. E. I. Ramakers, J. C. M. van Hesta, and D. W. P. M. Löwik, *Chem. Soc. Rev.*, 2014, **43**, 2743.
65 E. D. Santis and M. G. Ryadnov, *Chem. Soc. Rev.*, 2015, **44**, 8288.
66 D. M. Raymonda and B. L. Nilsson, *Chem. Soc. Rev.*, 2018, 10.1039/C8CS00115D.
67 Q. Luo, C. Hou, Y. Bai, R. Wang, and J. Liu, *Chem. Rev.*, 2016, **116**, 13571.
68 K. Oohora, A. Onoda, and T. Hayashi, *Chem. Commun.*, 2012, **48**, 11714.
69 A. Ikeda and S. Shinkai, *Chem. Rev.*, 1997, **97**, 1713.
70 K. Helttunena and P. Shahgaldian, *New J. Chem.*, 2010, **34**, 2704.
71 S. Fujii, S. Yamada, S. Matsumoto, G. Kubo, K. Yoshida, E. Tabata, R. Miyake, Y. Sanada, I. Akiba, T. Okobira, N. Yagi, E. Mylonas, N. Ohta, H. Sekiguchi, and K. Sakurai, *Sci. Rep.*, 2017, **7**, 44494.
72 S. Pasquale, S. Sattin, Eduardo. C. Escudero-Adán, M. Martínez-Belmonte, and J. de Mendoza, *Nat. Commun.*, 2012, **3**, 785.
73 Y. Aoyama, *Chem. Eur. J.*, 2004, **10**, 588.
74 Y. Aoyama, Trends Glycosci. Glycotech., 2005, **17**, 39.
75 O. Hayashida, K. Mizuki, K. Akagi, T. Nakai, S. Sando, and Y. Aoyama, *J. Am. Chem. Soc.*, 2003, **125**, 594.
76 Y. Aoyama, T. Kanamori, T. Nakai, T. Sasaki, S. Horiuchi, S. Sando, and T. Niidome, *J. Am. Chem. Soc.*, 2003, **125**, 3455.
77 T. Nakai, T. Kanamori, S. Sando, and Y. Aoyama, *J. Am. Chem. Soc.*, 2003, **125**, 8465.
78 K. Matsuura, K. Murasato, and N. Kimizuka, *J. Am. Chem. Soc.*, 2005, **127**, 10148.
79 K. Murasato, K. Matsuura, and N. Kimizuka, *Biomacromolecules*, 2008, **9**, 913.
80 A. G. Cochran, N. J. Skelton, and M. A. Starovasnik, *Proc. Natl. Acad. Sci. USA*, 2001, **98**, 5578.
81 W. W. Streicher and G. I. Makhatadze, *J. Am. Chem. Soc.*, 2006, **128**, 30.

82 E. C. Dempsey, T. J. Piggot, and P. E. Mason, *Biochemistry*, 2005, **44**, 775.
83 K. Matsuura, H. Hayashi, K. Murasato, and N. Kimizuka, *Chem. Commun.*, 2011, **47**, 265.
84 V. Castelletto, E. D. Santis, H. Alkassem, B. Lamarre, J. E. Noble, S. Ray, A. Bella, J. R. Burns, B. W. Hoogenboom, and M. G. Ryadnov, *Chem. Sci.*, 2016, **7**, 1707.
85 M. Reches and E. Gazit, *Science*, 2003, **300**, 625.
86 E. Gazit, *Chem. Soc. Rev.*, 2007, **36**, 1263.
87 R. P. Lyon and W. M. Atkins, *J. Am. Chem. Soc.*, 2001, **123**, 4408.
88 S. S. Mahajan, R. Paranji, R. Mehta, R. P. Lyon, and W. M. Atkins, *Bioconjugate Chem.* 2005, **16**, 1019.
89 K. Matsuura, H. Matsuyama, T. Fukuda, K. Murasato, and N. Kimizuka, *Soft Matter*, 2009, **5**, 2463.
90 K. Matsuura, K. Tochio, K. Watanabe, and N. Kimizuka, *Chem. Lett.*, 2011, **40**, 711.
91 K. Matsuura, K. Fujino, T. Teramoto, K. Murasato, and N. Kimizuka, *Bull. Chem. Soc. Jpn.*, 2010, **83**, 880.
92 S. Ghosh, M. Reches, E. Gazit and S.Verma, *Angew. Chem. Int. Ed.*, 2007, **46**, 2002.
93 H. R. Marsden and A. Kros, *Angew. Chem. Int. Ed.*, 2010, **49**, 2988.
94 N. Kobayashi, K. Yanase, T. Sato, S. Unzai, M. H. Hecht, and R. Arai, *J. Am. Chem. Soc.*, 2015, **137**, 11285.
95 H. Gradišar, S. Božič, T. Doles, D. Vengust, I. Hafner-Bratkovič, A. Mertelj, B. Webb, A. Šali, S. Klavžar and R. Jerala, *Nat. Chem. Biol.*, 2013, **9**, 362.
96 A. Ljubetič, F. Lapenta, H. Gradišar, I. Drobnak, J. Aupič, Ž. Strmšek, D. Lainšček, I. Hafner-Bratkovič, A. Majerle, N. Krivec, M. Benčina, T. Pisanski, T. Ć. Veličković, A. Round, J. M. Carazo, R. Melero, and R. Jerala, *Nat. Biotech.*, 2017, **35**, 1094.
97 A. Ljubetič, I. Drobnak, H. Gradišarab and R. Jerala, *Chem. Commun.*, 2016, **52**, 5220.
98 F. Boato, R. M. Thomas, A. Ghasparian, A. Freund-Renard, K. Moehle, and J. A. Robinson, *Angew. Chem. Int. Ed.*, 2007, **46**, 9015.
99 J. E. Noble, E. De Santis, J. Ravi, B. Lamarre, V. Castelletto, J. Mantell, S. Ray, and M. G. Ryadnov, *J. Am. Chem. Soc.*, 2016, **138**, 12202.
100 J. M. Fletcher, R. L. Harniman, Fr. R. H. Barnes, A. L. Boyle, A. Collins, J. Mantell, T. H. Sharp, M. Antognozzi, P. J. Booth, N. Linden, M. J. Miles, R. B. Sessions, P. Verkade, and D. N. Woolfson, *Science*, 2013, **340**, 595.
101 E. De Santis, H. Alkassem, B. Lamarre, N. Faruqui, A. Bella, J. E. Noble, N. Micale, S. Ray, J. R. Burns, A. R. Yon, B. W. Hoogenboom and M. G. Ryadnov, *Nat. Commun.*, 2017, **8**, 2263.
102 P. S. Satheshkumar, G. L. Lokesh, M. R Murthy, H. S. Savithiri, *J. Mol. Biol.*, 2005, **353**, 447.
103 S. B. Larson, J. Day, M. A. Canady, A. Greenwood, A. McPherson, *J. Mol. Biol.*, 2000, **301**, 625.
104 P. Plevka, K. Tars, A. Zeltins, I. Balke, E. Truve, L. Liljas, *Virology*, 2007, **369**, 364.
105 U. Katpally, K. Kakani, R. Reade, K. Dryden, D. Rochon, T. J. Smith, *J. Mol. Biol.*, 2007, **365**, 502.
106 Y. Oda, K. Saeki, Y. Takahashi, T. Maeda, H. Naitow, T. Tsukihara, K. Fukuyama, *J. Mol. Biol.*, 2000, **300**, 153.
107 J. D. Powell, E. Barbar, T. W. Dreher, *Virology*, 2012, **422**, 165.
108 K. Matsuura, K. Watanabe, K. Sakurai, T. Matsuzaki, and N. Kimizuka, *Angew. Chem. Int. Ed.*, 2010, **49**, 9662.
109 K. Matsuura, Y. Mizuguchi, and N. Kimizuka, *Biopolymers: Pept. Sci.*, 2016, **106**, 470.
110 K. Matsuura, K. Watanabe, Y. Matsushita, and N. Kimizuka, *Polymer J.*, 2013, **45**, 529.
111 S. Fujita and K. Matsuura, *Chem. Lett.*, 2016, **45**, 922.
112 K. Matsuura, T. Nakamura, K. Watanabe, T. Noguchi, K. Minamihata, N. Kamiya, and N. Kimizuka, *Org. Biomol. Chem.*, 2016, **14**, 7869.
113 S. Fujita and K. Matsuura, *Nanomaterials*, 2014, **4**, 778.
114 K. Matsuura, G. Ueno, and S. Fujita, *Polymer J.*, 2015, **47**, 146.
115 Y. Nakamura, S. Yamada, S. Nishikawa, and K. Matsuura, *J. Pept. Sci.*, 2017, **23**, 636.
116 S. Fujita and K. Matsuura, *Org. Biomol. Chem.*, 2017, **15**, 5070.
117 J. E. Padilla, C. Colovos, and T. O. Yeates, *Proc. Nat. Acad. Sci., USA*. 2001, **98**, 2217.
118 Y. T. Lai, D. Cascio and T. O. Yeates, *Science*, 2012, **336**, 1129.
119 Y. T. Lai, K. L. Tsai, M. R. Sawaya, F. J. Asturias, and T. O. Yeates, *J. Am. Chem. Soc.*, 2013, **135,** 7738.
120 Y. T. Lai, E. Reading, G. L. Hura, K.-L. Tsai, A. Laganowsky, F. J. Asturias, J. A. Tainer, C. V. Robinson, and T. O. Yeates, *Nat. Chem.*, 2014, **6**, 1065.
121 Y. Hsia, J. B. Bale, S. Gonen, D. Shi, W. Sheffler, K. K. Fong, U. Nattermann, C.Xu, P.-S. Huang, R. Ravichandran, S. Yi, T. N. Davis, T. Gonen, N. P. King, and D. Baker, *Nature*, 2016, **535**, 136.
122 J. B. Bale, S. Gonen, Y. Liu, W. Sheffler, D. Ellis, C. Thomas, D. Cascio, T. O. Yeates, T. Gonen, N. P. King, and D. Baker, *Science*, 2016, **353**, 389.
123 A. K. Khan, S. Gudlur, H.-P. M. de Hoog, W. Siti, B. Liedberg, and M. Nallani, *Angew. Chem. Int. Ed.*, 2017, **56**, 11754.
124 S. Katen and A. Zlotnick, *Methods Enzymol.*, 2009, **455**, 395–417.
125 Z. Tan, M. L. Maguire, D. D. Loeb, and A. Zlotnick, *J. Virol.*, 2013, **87**, 3208–3216.
126 R. F. Garmann, M. Comas-Garcia, C. M. Knobler, and W. M. Gelbart, *Acc. Chem. Res.*, 2016, **49**, 48-55.
127 S. D. Perrault and W. M. Shih, *ACS Nano*, 2014, **8**, 5132.
128 J. Votteler, C. Ogohara, S. Yi, Y. Hsia, U. Nattermann, D. M. Belnap, N. P. King, and W. I. Sundquist, *Nature*, 2016, **540**, 292.
129 S. Nakano, D. Miyoshi, and N. Sugimoto, *Chem. Rev.*, 2014, **114**, 2733.